Geoderma 412 (2022) 115716

Contents lists available at ScienceDirect

Geoderma

journal homepage: www.elsevier.com/locate/geoderma

The molecular size continuum of soil organic phosphorus and its chemical associations

Jolanda E. Reusser [a,d,*], Federica Tamburini [a], Andrew L. Neal [b], René Verel [c], Emmanuel Frossard [a], Timothy I. McLaren [a]

[a] Department of Environmental Systems Science, ETH Zurich, CH-8315 Lindau, Switzerland
[b] Department of Sustainable Agriculture Sciences, Rothamsted Research, North Wyke, Devon EX20 2SB, United Kingdom
[c] Department of Chemistry and Applied Biosciences, ETH Zurich, CH-8093 Zurich, Switzerland
[d] Swiss Soil Monitoring Network (NABO), Agroscope, CH-8046 Zurich, Switzerland

ARTICLE INFO

Handling Editor: Ingrid Kögel-Knabner

Keywords:
Organic phosphorus
High molecular weight
Soil organic matter
Inositol phosphates
Solution NMR spectroscopy
Phytate

ABSTRACT

The chemical nature of most organic P (P_{org}) in soil remains 'unresolved' but is accounted for by a broad signal in the phosphomonoester region of solution ^{31}P nuclear magnetic resonance (NMR) spectra. The molecular size range of this broad NMR signal and its molecular structure remain unclear. The aim of this study was to elucidate the chemical nature of P_{org} with increasing molecular size in soil extracts combining size exclusion chromatography (SEC) with solution ^{31}P NMR spectroscopy. Gel-filtration SEC was carried out on NaOH-EDTA extracts of four soils (range 238–1135 mg P_{org}/kg_{soil}) to collect fractions with molecular sizes of < 5, 5–10, 10–20, 20–50, 50–70, and > 70 kDa. These were then analysed by NMR spectroscopy.

Organic P was detected across the entire molecular size continuum from < 5 to > 70 kDa. Concentrations of P_{org} in the > 10 kDa fraction ranged from 107 to 427 mg P/kg_{soil} and exhibited on average three to four broad signals in the phosphomonoester region of NMR spectra. These broad signals were most prominent in the 10–20 and 20–50 kDa fractions, accounting for on average 77 % and 74 % of total phosphomonoesters, respectively. Our study demonstrates that the broad signals are present in all investigated molecular size fractions and comprise on average three to four components of varying NMR peak line width (20 to 250 Hz).

The stereoisomers *myo*- and *scyllo*-inositol hexakisphosphates (IP_6) were also present across multiple molecular size ranges but were predominant in the 5–10 kDa fraction. The proportion of IP associated with large molecular size fractions > 10 kDa was on average 23 % (SD = 39 %) of total IP across all soils. These findings suggest that stabilisation of IP in soil includes processes associated with the organic phase.

1. Introduction

Phosphorus (P) is an innate constituent of soil organic matter. Pools of organic P (P_{org}) typically comprise between 20 % and 80 % of total P ($P_{tot,s}$) in most soils (Anderson, 1980; Harrison, 1987). Inositol phosphates (IP) are an abundant and relatively stable pool of P_{org} in soil (Turner et al., 2002): the *myo* stereoisomer of IP_6 is typically the most abundant form and comprises on average one third of the soil P_{org} (McLaren et al., 2020). *myo*-IP_6 accumulates in soil, largely due to its high sorption affinity to soil components, e.g. iron (Fe) and aluminium (Al) oxides, calcium (Ca) carbonates, clay surfaces and organic matter (Celi and Barberis, 2007). Such sorption as well as complexation with metal cations (Martin and Evans, 1987) limit the accessibility of IP to enzymatic hydrolysis (Celi and Barberis, 2005; Celi and Barberis, 2007). Other identifiable pools of P_{org} include phosphonates (e.g. 2-aminoethylphosphonate), nucleic acids (e.g. DNA and RNA) and phospholipids. These generally account for < 10 % of soil $P_{tot,s}$ (Anderson and Malcolm, 1974; Dalal, 1977) due to their rapid microbial degradation (Auten, 1923; Harrison, 1982). The chemical nature of > 50 % of soil P_{org} remains unresolved and consequently the mechanisms controlling its flux in the soil–plant system are still poorly understood (McLaren et al., 2020).

Several studies have shown that large proportions of P_{org} in soil extracts occur in large molecular weight material above 10 kDa. Moyer and Thomas (1970) reported that 31 % of extractable P_{org} from a Luvisol had a molecular weight range of 1–50 kDa, whereas 36 % of the

* Corresponding author.
E-mail address: jolanda.reusser@agroscope.admin.ch (J.E. Reusser).

https://doi.org/10.1016/j.geoderma.2022.115716
Received 23 July 2021; Received in revised form 12 January 2022; Accepted 12 January 2022

extractable P_{org} had a molecular weight range > 50 kDa. Steward and Tate (1971) reported that the majority of extractable P_{org} from several alkaline soils had a molecular weight range > 30 kDa. Large pools of P_{org} present in high molecular weight material have been reported in several review papers (Anderson, 1980; Kögel-Knabner and Rumpel, 2018; McLaren et al., 2020). However, there is limited information on the chemical nature of P_{org} with increasing molecular weight. Some studies provide evidence supporting the existence of IP in high molecular weight material (Borie et al., 1989; Hong and Yamane, 1981; Moyer and Thomas, 1970), despite the molecular size of IP being about 660 Da or less. These studies often suggest that the presence of IP in high molecular weight material could be due to a polymeric form of IP, or IP bound to (or within) other organic compounds. In this latter case, it is proposed that IP might be complexed to organic compounds via polyvalent metals, such as Fe and Al (Lévesque, 1969; Lévesque and Schnitzer, 1967; Veinot and Thomas, 1972).

With the advent of solution ^{31}P NMR spectroscopy on soil extracts in the 1980s (Newman and Tate, 1980), it was possible to simultaneously detect diverse organic P compounds in soil extracts (Doolette and Smernik, 2011). However, with NMR becoming the commonly applied organic P speciation technique, the focus of soil organic P research shifted towards the identification and quantification of sharp peaks in NMR spectra arising from relatively small molecules such as inositol phosphates; phospholipids and phosphonates (Cade-Menun, 2015; Turner et al., 2012; Turner et al., 2003; Turner and Richardson, 2004; Vestergren et al., 2012). Research on the high molecular weight P_{org} pool reported in the 'chromatography-era' as defined by McLaren et al. (2020) was neglected until Dougherty et al. (2007) reported the presence of an underlying broad feature in the phosphomonoester region of ^{31}P NMR soil spectra. Bünemann et al. (2008) integrated this feature in the spectral deconvolution fitting method and reported that whilst this broad signal was present in soil extracts of a Chromic Luvisol resp. a Calcisol, it was absent in model soils.

In general, the largest pool of soil P_{org} is observed as an underlying broad signal in the phosphomonoester region of solution ^{31}P NMR spectra of soil extracts (Doolette et al., 2011; Jarosch et al., 2015; McLaren et al., 2015). Despite the high abundance and hence importance in the soil P cycle, little is known about the availability of this P_{org} pool for plant nutrition. Due to its correlation with P compounds resistant to enzymatic hydrolysis, Jarosch et al. (2015) suggested the P_{org} pool causing the underlying broad signal had a high stability against enzymatic attack. Furthermore, Annaheim et al. (2015) reported that concentrations of the compounds responsible for the underlying broad signal did not change after 62 years of cropping in field trials investigating three different fertiliser strategies whereas added P_{org} compounds were completely transformed or lost. A better understanding of the chemical and structural composition of this highly abundant P_{org} pool is needed in order to investigate its behaviour and stability in the soil–plant system.

Compounds responsible for the broad signal typically comprise 40–70 % of total P_{org} and are of an apparent high molecular weight. Jarosch et al. (2015) used Sephadex G-25 gel to separate NaOH-EDTA extracts according to molecular size from several soils. The authors found that P_{org} was detected in both low (< 5 kDa) and high (> 5 kDa) size fractions. Pools of P_{org} in the latter fraction were largely stable to enzymatic hydrolysis and correlated with pools of phosphomonoesters exhibiting a broad NMR signal. At the same time, McLaren et al. (2015) used ultrafiltration to separate NaOH-EDTA extracts from diverse soils into < 10 kDa and > 10 kDa fractions. These authors reported that about 32 % of P_{org} was measured in the larger fraction, and was dominated by a broad NMR signal in the phosphomonoester region. However, the authors also reported the presence of a broad signal in the phosphomonoester region of NMR spectra of < 10 kDa fractions.

The structural composition of the broad signal in the phosphomonoester region of solution ^{31}P NMR spectra on soil extracts was later investigated by McLaren et al. (2019) using transverse relaxation (T_2) experiments. The authors found that T_2 times associated with the broad signal were considerably shorter than those of sharp signals (e.g. *myo*-IP_6) in the phosphomonoester region, suggestive of the former having a large molecular size (Bloembergen et al., 1948; Keeler, 2010). This was similarly the case for T_2 experiments carried out on soil extracts following hypobromite oxidation (Reusser et al. (2020b). McLaren et al. (2019) compared the line width of the broad signal at half peak intensity based on spectral deconvolution with that derived from T_2 experiments. The authors reported that the line width at half peak intensity of the broad signal based on the former approach was significantly larger than that based on the latter approach, suggesting the broad signal itself is derived from multiple components. The number of components and their chemical composition remains unknown.

Organic compounds containing phosphate in soil are known for their capacity to form complexes with metal cations, such as Al and Fe (Parfitt, 1979; Stevenson, 1994; Turner et al., 2002; Vincent et al., 2012). Such complexes of soil organic matter (SOM) and P_{org} (i.e. IP) with metals contribute to the stabilisation and possible accumulation of organic compounds in soil (Celi and Barberis, 2005; Stevenson, 1994). Gerke (2010) reported that orthophosphate is not directly bound to an organic moiety of SOM, as would be the case for P_{org} compounds, but indirectly associated with the SOM via metal bridges. The authors identified Al^{3+} and Fe^{3+} as the predominant metal linkages in humic-metal-P complexes.

The aim of this study was to provide new insight on the chemical nature of P_{org} at increasing molecular size in soil extracts, combining size exclusion chromatography (SEC) and solution ^{31}P NMR spectroscopy. We hypothesised that: 1) phosphomonoesters in large molecular size material are dominated by several broad signals in the phosphomonoester region, but also contain several sharp signals due to IP; 2) the composition, and hence the peak shape and intensity of the underlying broad signal in the phosphomonoester region of ^{31}P NMR soil spectra, will change among molecular size fractions; and 3) concentrations of Fe and Al in large molecular size material will correlate with that of IP, indicating the importance of metals in bridging IP with large molecular size compounds.

This study bridges research on small identifiable P_{org} molecules, such as lower-order IP (Reusser et al., 2020b), with research on colloid-associated P (Missong et al., 2016).

2. Experimental section

2.1. Soil collection and preparation

The A horizon of a Cambisol pasture (P) soil from Switzerland, a Cambisol forest (F) soil from Germany, a Gleysol pasture soil and an arable (A) Cambisol soil from Switzerland (WRB, 2014) were investigated in this study. These soil samples were chosen out of a collection of six soil samples (Reusser et al., 2020a) based on their diverse composition of the phosphomonoester region in ^{31}P NMR soil spectra and elevated concentrations of P_{org}. Detailed information of sampling sites, cropping systems and properties of the four soils can be found in Reusser et al. (2020a). Additional information on oxalate extractable concentrations of total Fe, Al, and P are reported in Table 1. For each, 1 g of soil was extracted with 100 mL of 0.2 M acid oxalate solution (Tamm-reagent at pH 3) according to the modified method of Schwertmann

Table 1
Oxalate extractable aluminium, iron and phosphorus of the soil samples reported in this study.

Soil	Al_{ox}(g Al/kg_{soil})	Fe_{ox}(g Fe/kg_{soil})	P_{ox}(mg P/kg_{soil})
Cambisol (P)	1.5	3.4	643.4
Cambisol (F)	7.2	48.8	1795.0
Gleysol	3.2	3.5	989.3
Cambisol (A)	0.8	2.0	337.0

(1964), as described in Pansu and Gautheyrou (2006). Tubes were shaken end-over-end for 4 h at 11 revolutions per min in the absence of light at 20 °C, centrifuged at 6480 *g* for 10 min, and the supernatant analysed for total Al, Fe and P using inductively coupled plasma-optical emission spectroscopy (ICP-OES).

2.2. Concentrations of total phosphorus in soil

Microwave acid digestion was used to determine the concentration of $P_{tot,s}$ in soil based on the method of Fioroto et al. (2017). In brief, 200 mg of dried and ground soil was digested in 4 mL of a 14 M nitric acid solution using a turboWAVE® MRT microwave digestion system (MILESTONE Srl, Sorisole, Italy) at 250 °C for 35 min. The digestate was then diluted to 10 mL with deionised water and analysed for P using the malachite green method of Ohno and Zibilske (1991).

2.3. Extraction of soil organic phosphorus

Extraction of P_{org} from soil was based on the method of Cade-Menun et al. (2002). Briefly, 4 g of soil was extracted with 40 mL of 0.25 M NaOH + 0.05 M EDTA (NaOH-EDTA) solution and shaken for 16 h. The tube was then centrifuged at 4643 *g* for 10 min and the supernatant filtered through a Whatman no. 42 filter paper. Concentrations of total P in soil filtrates ($P_{tot,e}$) were determined by ICP-OES. Concentrations of molybdate reactive P (MRP) in soil filtrates were measured using the malachite green method (Ohno and Zibilske, 1991). Molybdate reactive P is considered to represent inorganic P (P_{inorg}) in the extract. The difference in concentrations of $P_{tot,e}$ and MRP is referred to as molybdate unreactive P (MUP), conventionally considered to be P_{org} (Bowman and Moir, 1993).

2.4. Size-exclusion chromatography

A summary of the extraction, fractionation and analyses steps is illustrated schematically in Figure SI-1. Initially, we carried out high-pressure liquid (HPL)-SEC with in-line inductively coupled plasma-mass spectrometry (ICP-MS) on lyophilised NaOH-EDTA soil extracts based on the method of Dell'Aquila et al. (2020) at Rothamsted Research (supporting information). Separation of samples was performed via SEC using an HPLC (PerkinElmer LC 200 Series HS, Seer Green, Bucks, UK) composed of an injector, a Flexar UV/VIS detector operating at 280 nm and a high-pressure peristaltic pump equipped with PEEK tubing (0.17 mm internal diameter), operated at a flow rate of 0.6 mL/min. Samples were analysed using an ICP-MS (PerkinElmer NexION 300XX, Seer Green, Bucks, UK) equipped with a glass Meinhard nebuliser, a quadrupole mass spectrometer and a collision cell. The column was a Superdex Peptide 10/300 GL (10 mm diameter × 300 mm length, GE Healthcare Bio-Sciences, Sweden). This revealed well resolved chromatograms with a continuum of P spanning the < 1 to > 20 kDa molecular size range (Figures SI-3 and SI-4). Concentrations of P in collections of discrete molecular size fractions were too low for P characterisation using NMR spectroscopy. An alternative preparative SEC method (i.e. high-resolution SEC) was used to fractionate NaOH-EDTA soil extracts according to molecular size which yielded sufficient concentrations of P in collected solution volumes for characterisation using NMR spectroscopy.

To prepare the soil extracts for size-fraction collection by high-resolution SEC, salts were first removed. This preparatory desalting procedure resulted in separation of soil filtrates into two size fractions with molecular sizes of < 5 kDa and > 5 kDa, based on a modified version of the method of Jarosch et al. (2015). Soils were extracted with NaOH-EDTA as described above. A 15 mL aliquot of soil filtrate was diluted with 35 mL of deionised water and filtered through a 0.22 μm syringe filter: the Cambisol (F) was filtered using a 0.45 μm syringe filter due to blockage of 0.22 μm syringe filters. Desalting of the filtrate was carried out on an ÄKTAprime plus system (GE Healthcare), using a 4.5 cm (diameter) × 16 cm (length) column filled with Sephadex™ G-25 (GE Healthcare) with an exclusion limit of 5 kDa. The injected sample was eluted with deionised water at a flow rate of 1 mL/min and an upper-limit pressure of 0.2 MPa. Runtime was about 360 min and carried out under constant temperature (4 °C). The eluate was collected in 9 mL fractions. The cut-off at 5 kDa was defined based on the conductivity (peak indicating eluted orthophosphate ions), the absorbance (two major peaks) and measured concentrations of P_{inorg} and P_{org} in the collected fractions (Tamburini et al., 2018). The absorbance and conductivity curves with the determined cut-off are plotted in Figures SI-6 and SI-7 in the supporting information. Subsamples with molecular sizes > 5 kDa were combined (total volume of 126–135 mL) and lyophilised. Similarly, subsamples with molecular sizes < 5 kDa were combined (total volume of 117–135 mL) and lyophilised.

High-resolution SEC was carried out to collect fractions of P_{org} across a wide molecular size distribution, which could then be analysed using solution ^{31}P NMR spectroscopy. The lyophilised material of the desalted soil extracts (> 5 kDa fraction) was redissolved in 10 mL of deionised water. A 4 mL aliquot was then injected onto a 1.6 cm (diameter) × 68.2 cm (length) column containing Superdex™ 75 prep grade resin beads (GE Healthcare) with a fractionation range of ~ 3 to 70 kDa (globular proteins). The sample was eluted with degassed 0.2 M ammonium nitrate (pH approx. 7.6) at a flow rate of 0.5 mL/min and a pump pressure of 0.3 MPa. Runtime for each sample was about 300 min and carried out under constant temperature (4 °C). As soon as the UV/VIS detector measured an increase in absorbance, 1 mL subsamples were collected.

The sensitivity curve of the column was calculated in the same way as described for the HPL-SEC analysis in the supporting information (Figure SI-2) but using a standard mixture of vitamin B_{12} (0.24 mg/mL), aprotinin (0.92 mg/mL), myoglobin (0.98 mg/L), albumin (1.44 mg/L) and blue dextran (1.16 mg/mL). Based on the sensitivity curve, and information provided from HPL-SEC analysis, elution times corresponding to molecular size cut-offs of 5 kDa, 10 kDa, 20 kDa, 50 kDa and 70 kDa were chosen. Subsamples were combined accordingly, resulting in molecular size fractions of < 5 kDa (28–30 mL), 5–10 kDa (14 mL), 10–20 kDa (14 mL), 20–50 kDa (18 mL), 50–70 kDa (7 mL) and > 70 kDa (14–18 mL). For the Cambisol (P) soil, the 50–70 kDa and > 70 kDa fractions were combined due to a preparation error. A 450 μL aliquot was taken from each fraction in order to determine the concentration of MRP using the malachite green method (Ohno and Zibilske, 1991), and concentrations of total P, Fe, Al, Mn, Ca and K were determined using ICP-OES. The remaining volume of each collected fraction was lyophilised prior to NMR sample preparation, resulting in 90 to 440 mg of lyophilised material.

2.5. Sample preparation for solution ^{31}P NMR spectroscopy

Sample preparation for NMR analyses was carried out based on the methods of Spain et al. (2018) and Reusser et al. (2020a). Lyophilised material from each fraction was redissolved in 600 μL of NaOH-EDTA (a concentration factor of 13.55), except for the 10–20 kDa fraction of the Cambisol (F) which had a concentration factor of 18.55, when compared to the pre-lyophilisation volume. The solution was stored overnight to allow for complete hydrolysis of RNA and phospholipids (Vestergren et al., 2012), and then centrifuged at 10621 *g* for 15 min at 21 °C. A 500 μL aliquot of the supernatant was transferred to a 1.5 mL microcentrifuge tube and spiked with 25 μL sodium deuteroxide (NaOD) at 40 % (w/w) in D_2O (Sigma-Aldrich, product no. 372072) and 25 μL of a 0.03 M methylenediphosphonic acid standard (MDP) made up in D_2O (Sigma-Aldrich, product no. M9508). The prepared solution was then homogenised with a vortex mixer and transferred to a 5 mm NMR tube.

The fraction removed by the desalting process (< 5 kDa), which was not subjected to high-resolution SEC, was prepared by redissolving 150 mg of lyophilised material with 750 μL of NaOH-EDTA. This was then stored and centrifuged as above. A 125 μL aliquot of the supernatant was diluted with 9.875 mL of deionised water and subsequently analysed for

P and metals as described above. A 500 µL aliquot of the remaining supernatant was transferred to a 1.5 mL microcentrifuge tube. The supernatant was further prepared for NMR analysis as described above, except that 35 µL of NaOD was used instead of 25 µL to adjust the chemical shift of the orthophosphate peak. Furthermore, the Cambisol (F) and Gleysol samples were diluted with an additional 300 µL of NaOH-EDTA in the NMR tube due to considerable line broadening, which resolved the issue.

2.6. Solution ^{31}P NMR analysis and processing of spectra

Detailed information on the solution ^{31}P NMR analyses and processing of NMR spectra can be found in McLaren et al. (2019) and Reusser et al. (2020a). Spectra were acquired using a Bruker 500 MHz NMR spectrometer (^{31}P frequency of 202.5 MHz) equipped with a Prodigy CryoProbe™ (Bruker Corporation, Billerica, USA). Inverse gated proton decoupling (90° pulse of 12 µs) was applied. Longitudinal relaxation (T_1) times were determined for each sample based on a preliminary inversion recovery experiment (Vold et al., 1968), which involved a recycle delay of 5 s and 24 scans per experiment. Longitudinal relaxation values were calculated from 10 individual experiments with increasing time periods ranging from 5 to 400 ms between the applied pulses (total analysis time was 56 min per sample). These experiments indicated recycle delays (i.e. five times T_1 of the slowest NMR signal) ranging from 5.5 to 33.0 s across all samples. Solution 1D ^{31}P NMR analyses were carried out with 4096 scans for each sample.

NMR spectra were processed (phase correction, baseline adjustment and integration) using the TopSpin® software environment (Bruker Corporation, Billerica, USA). Spectra are presented with a common line broadening of 0.6 Hz. For quantification of P species, spectral integration was performed. Relative proportions of peak regions compared to the net peak area of the MDP standard (δ 17.45 to 16.06 ppm), which has a known P concentration, were calculated for all samples (Doolette et al., 2011; Turner, 2008). Peak regions included: 1) phosphonates (δ 20.14 to 16.41 ppm); 2) a combined orthophosphate and phosphomonoester region (δ 6.39 to 3.05 ppm); 3) phosphodiesters (δ 1.08 to −2.78 ppm), and 5) pyrophosphates (δ −4.12 to −5.48 ppm). The NMR observability for $P_{tot,e}$ in NaOH-EDTA extracts was determined for all samples by comparing the proportion of $P_{tot,e}$ as measured by NMR spectroscopy with that measured by ICP-OES (Doolette et al., 2011; Dougherty et al., 2005).

2.7. Spectral deconvolution fitting procedure

Spectral deconvolution fitting (SDF) was applied to the combined orthophosphate and phosphomonoester region to separate overlapping peaks as described in Reusser et al. (2020a). Sharp peaks were fitted simultaneously with underlying broad signals using a non-linear optimisation algorithm in MATLAB® R2017a (The MathWorks, Inc.). Multiple broad signals were fitted based on a visual assessment of the peak distributions, to further minimise the residuals of the fitting procedure, and supporting evidence for multiple components in the literature (McLaren et al., 2019; Reusser et al., 2020a; Reusser et al., 2020b).

2.8. Statistical analysis and graphics

Figures of chromatograms and element plots were created in Microsoft® Excel 2016, whereas all NMR spectra were created using MATLAB® R2017a of The MathWorks Inc. Statistical analyses, including calculation of mean values, standard deviations (SD) and coefficients of determination (R^2) of certain measured parameters, were carried out in Microsoft® Excel 2016. Pearson correlation coefficients r were calculated in R, version 4.0.3 (R Core Team, 2020).

3. Results

3.1. Soil phosphorus

Concentrations of $P_{tot,s}$ in soil ranged from 864 to 2260 mg P/kg_{soil} (Table 2). Pools of NaOH-EDTA extractable $P_{tot,e}$ ranged from 41 % (Cambisol (A)) to 95 % (Cambisol (P)) of $P_{tot,s}$ in each soil. Concentrations of P_{org} in the extracts ranged from 238 mg P/kg_{soil} (Cambisol (A)) to 1135 mg P/kg_{soil} (Cambisol (F)), which comprised on average 67 % of $P_{tot,e}$ in NaOH-EDTA extracts.

3.2. Phosphorus concentrations in molecular size fractions

Concentrations of $P_{tot,e}$ in the combined molecular size fractions ranged from 189 (Cambisol (A)) to 706 mg P/kg_{soil} (Gleysol), as determined by high-resolution SEC and ICP-OES (Table 3). This accounted for an average 48 % of $P_{tot,e}$ assessed in unfractionated soil extracts. Concentrations of P_{org} in the combined molecular size fractions ranged from 182 (Cambisol (A)) to 678 mg P/kg_{soil} (Gleysol), as determined from the differences of $P_{tot,e}$ and MRP. Overall, the distribution of P_{org} across the molecular size fractions can be broadly separated into three main groups (Figure SI-8): 1) concentrations of P_{org} were predominant in molecular size fractions < 10 kDa (Cambisol (P) and Gleysol); 2) concentrations of P_{org} were evenly distributed across the molecular size fractions (Cambisol (A)); and 3) concentration of P_{org} were predominant in molecular size fractions > 70 kDa (Cambisol (F)).

Concentrations of P_{inorg} in the combined molecular size fractions were low (< 45 mg P/kg_{soil}), as determined by high-resolution SEC and NMR spectroscopy (Table 3). The majority of P_{inorg} was measured in the < 5 kDa fraction of the soil filtrate following the desalting preparation process (Figure SI-9, Table SI-1). The predominant P species in this fraction was orthophosphate, comprising between 85 % and 91 % of $P_{tot,e}$. This fraction also contained minor concentrations of P_{org} as phosphomonoesters, which comprised between 7 % and 13 % of $P_{tot,e}$.

3.3. Organic phosphorus speciation in molecular size fractions

Diverse NMR signals were evident across all molecular size fractions (Fig. 1 and Fig. 2, and Figure SI-10), the majority being found in the phosphomonoester region (δ 6.0 to 3.0 ppm) (Fig. 1, Fig. 2. This region exhibited two main spectral features: a multitude of sharp peaks arising largely from IP, which were predominant in the < 5 and 10 kDa fractions; and several broad signals arising from unidentified P_{org} compounds, which were predominant in the > 10 kDa fractions.

Concentrations of phosphomonoesters were highest in fractions < 10 kDa and ranged from 19 (< 5 kDa fraction Cambisol (A)) to 120 mg

Table 2
Concentrations of $P_{tot,s}$ in soil determined by acid digestion, and pools of 0.25 M NaOH + 0.05 M EDTA extractable P determined using the method of Cade-Menun et al. (2002). For the NaOH-EDTA extractable P, mean values ($n = 3$) are listed with standard deviations in parentheses.

Soil	Digestion	NaOH-EDTA extraction		
	$P_{tot,s}$(mg P/kg_{soil})	$P_{tot,e}$(mg P/kg_{soil})	MRP[a](mg P/kg_{soil})	MUP[b](mg P/kg_{soil})
Cambisol (P)	913	863 (13)	319 (14)	544 (20)
Cambisol (F)	2260	1626 (13)	491 (5)	1135 (17)
Gleysol	1763	1620 (49)	508 (18)	1113 (66)
Cambisol (A)	864	356 (11)	118 (2)	238 (9)

[a] Molybdate reactive P (MRP), considered to be largely P_{inorg} (Ohno and Zibilske, 1991).

[b] Molybdate unreactive P (MUP), considered to be largely P_{org} (Hens and Merckx, 2001; Ohno and Zibilske, 1991)

Table 3
Concentrations (mg P/kg_{soil}) of total P ($P_{tot,e}$) in each molecular size fraction as determined by ICP-OES, and the main P classes (orthophosphate, phosphomonoester, phosphodiester and other compounds, such as polyphosphates, pyrophosphates and phosphonates) as determined by solution ^{31}P NMR spectral deconvolution fitting. Molecular size fractions were obtained on NaOH-EDTA soil extracts using high-resolution SEC (Superdex™ 75 prep grade column). The proportion (%) of P to $P_{tot,e}$ in each molecular size fraction is reported in parentheses. The < 5 kDa fractions do not account for the fraction removed by the desalting process (Table SI-1).

	$P_{tot,e}$ ICP-OES	$P_{tot,e}$ NMR	Ortho-P	P-monoester	P-diester	other P comp.
	(mg P/kg_{soil})	(mg P/kg_{soil})	(mg P/kg_{soil})	(mg P/kg_{soil})	(mg P/kg_{soil})	(mg P/kg_{soil})
Cambisol (P)						
<5 kDa	190.4	143.3	18.9 (13)	115.9 (81)	0.0 (0)	8.4 (6)
5–10 kDa	124.7	81.2	0.0 (0)	79.3 (98)	0.2 (0)	1.7 (2)
10–20 kDa	46.4	29.4	0.0 (0)	26.9 (91)	1.2 (4)	1.3 (5)
20–50 kDa	39.7	23.0	0.0 (0)	20.7 (90)	1.1 (5)	1.2 (5)
50->70 kDa*	33.5	15.4	0.0 (0)	13.8 (90)	0.0 (0)	1.6 (10)
Cambisol (F)						
<5 kDa	108.9	68.5	24.5 (36)	42.4 (62)	0.0 (0)	1.6 (2)
5–10 kDa	133.5	87.4	0.0 (0)	80.1 (92)	4.1 (5)	3.2 (4)
10–20 kDa	86.2	49.9	5.2 (10)	39.9 (80)	3.4 (7)	1.6 (3)
20–50 kDa	93.4	51.9	5.0 (10)	36.4 (70)	9.0 (17)	1.6 (3)
50–70 kDa	50.7	22.5	3.2 (14)	15.5 (69)	2.0 (9)	1.8 (8)
>70 kDa	229.9	54.7	6.7 (12)	43.1 (79)	2.6 (5)	2.2 (4)
Gleysol						
<5 kDa	73.5	135.8	7.9 (6)	119.9 (88)	0.0 (0)	8.0 (6)
5–10 kDa	73.4	95.4	0.0 (0)	93.5 (98)	0.5 (1)	1.5 (2)
10–20 kDa	103.8	42.2	4.9 (12)	35.5 (84)	1.6 (4)	0.2 (0)
20–50 kDa	81.4	51.6	2.9 (6)	42.9 (83)	5.4 (10)	0.4 (1)
50–70 kDa	172.8	33.1	1.7 (5)	23.7 (72)	6.6 (20)	1.1 (3)
>70 kDa	201.5	20.1	0.0 (0)	14.9 (74)	5.2 (26)	0.0 (0)
Cambisol (A)						
<5 kDa	43.4	25.4	6.0 (24)	19.4 (76)	0.0 (0)	0.0 (0)
5–10 kDa	38.3	25.4	0.4 (2)	24.9 (98)	0.0 (0)	0.1 (0)
10–20 kDa	21.8	14.4	0.4 (3)	13.7 (96)	0.0 (0)	0.2 (2)
20–50 kDa	31.8	16.6	0.0 (0)	16.5 (99)	0.0 (0)	0.1 (1)
50–70 kDa	18.1	9.9	0.3 (3)	8.7 (87)	0.5 (5)	0.6 (6)
>70 kDa	36.0	9.4	0.0 (0)	7.4 (79)	1.8 (20)	0.1 (2)

* The 50–70 kDa and > 70 kDa fractions of Cambisol (P) have been pooled. The given values represent the concentrations measured in the pooled fraction.

P/kg_{soil} (< 5 kDa fraction Gleysol) (Table 3). Sharp signals due to *myo*- and *scyllo*-IP_6 were detected in the < 5 and 5–10 kDa fractions of the Cambisol (P) and Cambisol (A) (Table 4). In contrast, these two IP were prominent in several fractions of > 20 kDa for the Cambisol (F) and similarly for the Gleysol, but at lower concentrations (Table 4).

Concentrations of lower-IP in the combined molecular size fractions ranged from 2 (Cambisol (A)) to 16 mg P/kg_{soil} (Cambisol (P)) across all soils (Table 4). This included signals of *myo*-(1,2,4,5,6)-IP_5 in the < 5 and 5–10 kDa fractions of the Gleysol, *scyllo*-IP_5 in the < 5 kDa fractions of all soils and in all molecular size fractions of the Cambisol (F). Furthermore, traces (1.6 to 5.2 mg P/kg_{soil}) of *scyllo*-IP_4 were detected in the < 5 and 5–10 kDa fractions of the Cambisol (P) and in the 5–10 kDa of the Cambisol (F).

Several broad signals were present in the phosphomonoester region of all molecular size fractions and represented on average 64 % (SD = 20 %) of the total concentration of phosphomonoesters (Table 3, Table 4 and Figure SI-11). These broad signals were particularly prominent in the 10–20 and 20–50 kDa fractions, which comprised on average 77 % and 74 % of the total concentration of phosphomonoesters of each fraction, respectively. In contrast, their contribution to the total pool of phosphomonoesters was lowest in the < 5 kDa fraction but were still an important component (on average 44 %). Unlike the other soil samples, the broad signals dominated all size fractions of the Cambisol (A) soil extract. In this sample, on average 3.7 (SD = 1.9) broad peaks were fitted in the SDF procedure across all size fractions, whereas for other soil samples this was on average 2.0 (SD = 0.7) broad peaks. The average line width at half-height for each broad peak was 88 Hz (SD = 53). The half widths of the individual broad peaks decreased with increasing number of fitted broad peaks and were lowest in the Cambisol (A) (67, SD = 60), for which most underlying broad peaks were fitted.

Concentrations of phosphodiesters were highest in molecular size fractions above 10 kDa (Table 3). The peak associated with DNA was most prominent in the 20–50 kDa fraction of the Cambisol (F) and in the 50–70 kDa and > 70 kDa size fraction of the Gleysol, which comprised > 25 % of the total NMR signal (Table 3). Other P compounds including phosphonates and pyrophosphates comprised < 10 % of the total NMR signal (Table 3).

The NMR observability in the fraction removed by the desalting process (<5 kDa) was on average 91 %. In contrast, the NMR observability of the analysed molecular size fractions differed markedly: on average 27 % (SD = 1 %) in the > 70 kDa fraction, 48 % (SD = 4 %) in the 50–70 kDa fraction, 54 % (SD = 3 %) in the 20–50 kDa fraction, 60 % (SD = 5 %) in the 10–20 kDa fraction, 63 % (SD = 5 %) in the 5–10 kDa fraction and 66 % (SD = 6 %) in the < 5 kDa fraction.

4. Metal concentrations in molecular size fractions

In general, concentrations of Fe were highest in the < 5 and > 70 kDa molecular size fractions of all soils (Fig. 3). The ratio of Fe to Al in NaOH-EDTA extracts differed between soils and molecular size fractions. For the Cambisol (P), Al dominated the lowest size fraction, whereas Fe dominated the highest molecular size fraction. For the Gleysol, increasing concentrations of Fe were measured with increasing molecular size, not including the < 5 kDa fraction. The Cambisol (F) exhibited a similar distribution pattern of the Fe and Al concentrations across the molecular size fractions. For the Cambisol (A), Al was only detected in the highest molecular size fraction. This soil was alkaline with a pH of 7.7 measured in water (Meyer et al., 2017). In contrast, the pH of the other soil samples ranges from 3.6 (Cambisol (F)) to 5.1 (Cambisol (P)) (Reusser et al., 2020a). Concentrations of IP across all size fractions and soil samples were not significantly correlated with the measured Fe (r = 0.048, p = 0.829) or Al (r = 0.123, p = 0.576) concentrations. However, considering all molecular size fractions of the individual soils, IP concentrations were significantly positively correlated with Fe concentrations in the Cambisol (F) sample (r = 0.847, p = 0.033) and with Al concentrations in the Gleysol sample (r = 0.823, p = 0.044). These correlations were much less apparent in the other soils.

Calcium concentrations were highest in the < 5 kDa fraction for all soils and decreased rapidly with increasing molecular size.

5. Discussion

5.1. Phosphorus concentrations in molecular size fractions

The molecular weight distribution of P_{org} in soils has typically been studied using technically defined molecular weight fractions with cut-offs of either 5 kDa (Jarosch et al., 2015) or 10 kDa (McLaren et al., 2015). We present continuous molecular size distributions of extracted soil P. Our reported molecular size distribution of P ranges from small molecules < 5 kDa, i.e. orthophosphate, to large molecular size fractions > 5 kDa approaching nanoparticles (1–100 nm (Gottselig et al., 2017)). The quantitative results of P_{inorg} and P_{org} concentrations in

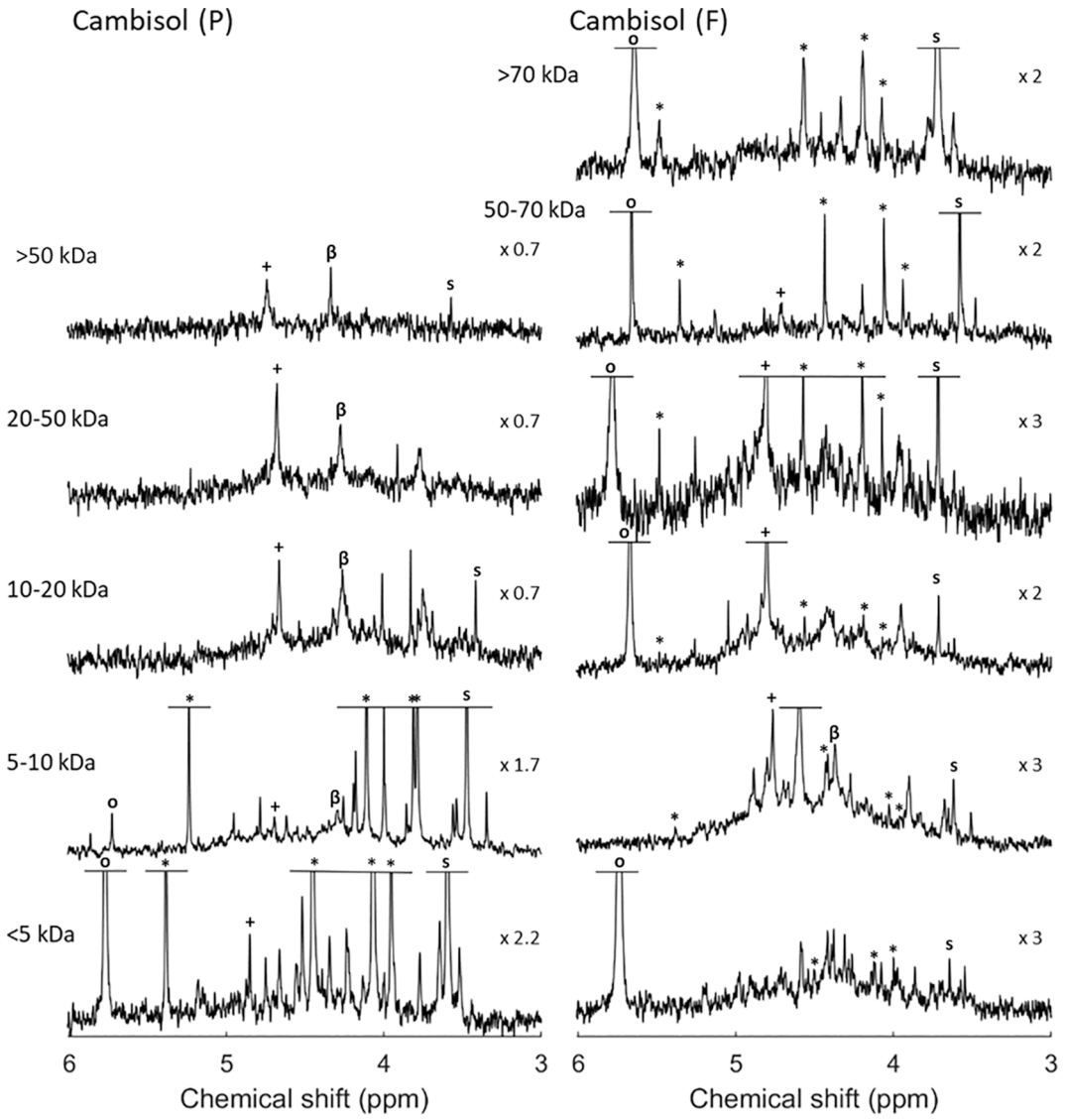

Fig. 1. Solution ^{31}P nuclear magnetic resonance (NMR) spectra (500 MHz) of the combined orthophosphate (**o**) and phosphomonoester region for each of six molecular size fractions generated from 0.25 M NaOH + 0.05 M EDTA soil extracts of the Cambisol (P) and Cambisol (F) soils (Superdex™ 75 prep grade column). Peaks associated with α-glycerophosphate/unknown high molecular weight P_{org} (McLaren et al., 2015) (+), β-glycerophosphate (**β**) as well as *myo*- (*) and *scyllo*- (**s**) IP_6 are marked. Signal intensities were normalised to a methylenediphosphonic acid standard peak intensity. The vertical axes were scaled for improved visibility of spectral features, as indicated by a factor. The molecular size fractions > 70 kDa and 50–70 kDa of the Cambisol (P) were pooled, shown as the > 50 kDa spectrum.

different molecular size fractions reported in this study confirm the previously proposed continuum of P across the molecular size distribution.

Pools of P_{org} exhibited a wide concentration range in the investigated soils (238 to 1135 mg P/kg_{soil}). Concentrations of NaOH-EDTA extractable P were similar to those reported in previous studies (Jarosch et al., 2015; McLaren et al., 2019). SEC chromatograms revealed a broad molecular size distribution of P in NaOH-EDTA extracts from soil. Furthermore, the majority of P_{org} was present in molecular size fractions > 5 kDa across all soils investigated here, despite differences in their chemical and physical properties. Several studies using SEC have reported that a large portion of P_{org} in soil extracts is detected in molecular size fractions above 10 kDa (Moyer and Thomas, 1970; Steward and Tate, 1971; Veinot and Thomas, 1972). The consistency and abundance of this high molecular size P_{org} pool in different soil systems suggests its importance in the soil P cycle.

5.2. Speciation of organic P compounds in molecular size fractions

Solution ^{31}P NMR spectroscopy on soil extracts revealed a large diversity of P compounds across all molecular size fractions and soil samples. Our results demonstrate a much greater diversity of organic P compounds across the molecular size continuum than was evident in previous studies (Jarosch et al., 2015; McLaren et al., 2015). In contrast to these studies, we were able to separate the > 10 kDa fraction further, showing that the distribution of different P_{org} compounds varied between large molecular size fractions > 10 kDa. Furthermore, the desalting preparation step resulted in improved resolution of the remaining peaks in the phosphomonoester region.

The molecular size material below 5 kDa was dominated by orthophosphate in the fraction removed by the desalting process and by phosphomonoesters in the < 5 kDa fraction of the subsequent high-resolution SEC. In the Cambisol (P) and Gleysol samples, the < 5 kDa fraction consisted mostly of IP, which were probably in the free form or desorbed from soil mineral surfaces (Celi and Barberis, 2007; Moyer and Thomas, 1970). The fraction removed by the desalting process (cut-off

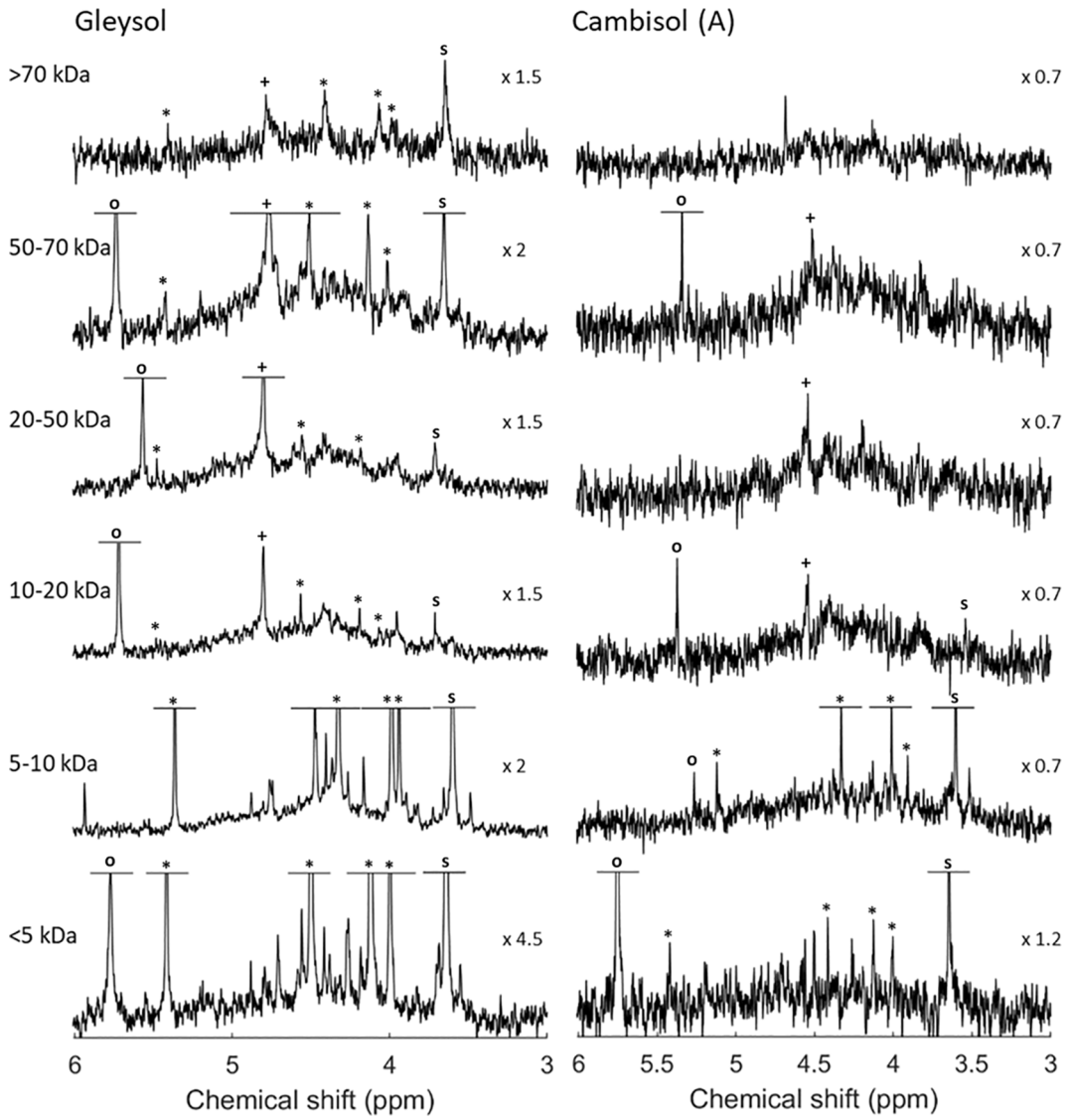

Fig. 2. Solution ^{31}P nuclear magnetic resonance (NMR) spectra (500 MHz) of the combined orthophosphate (**o**) and phosphomonoester region on the molecular size fractions (Superdex™ 75 prep grade column) of 0.25 M NaOH + 0.05 M EDTA soil extracts of the Gleysol and Cambisol (A). The peaks of α-glycerophosphate/unknown high molecular weight P_{org} (McLaren et al., 2015) (+) as well as *myo*- (*) and *scyllo*- (**s**) IP_6 are marked. Signal intensities were normalised to a methylenediphosphonic acid standard peak intensity. The vertical axes were scaled for improved visibility of spectral features, as indicated by a factor.

= 5 kDa) was less enriched in IP compared to the < 5 kDa fraction of the subsequent high-resolution SEC of the desalted extract, despite the molecular size of IP being 660 Da or less. Nebbioso and Piccolo (2012) reported that chromatographic separation weakens the supramolecular architecture of SOM. This may indicate that associations of IP with higher molecular size compounds were weakened during the desalting chromatography step but still eluted with the fraction above the cutoff, because the compounds already passed a certain distance in the column. Furthermore, the cutoff of the desalting process was set to the change in electric conductivity and UV absorbance in order to mainly remove salts and not organic compounds. The liberated IP may then have been eluted in the < 5 kDa fraction in the subsequent high-resolution SEC step.

Spectra derived from molecular size fractions > 5 kDa were dominated by poorly resolved broad ^{31}P NMR signals. Compounds causing these broad NMR signals are apparently of large molecular size. These findings are consistent with the studies of Jarosch et al. (2015) and McLaren et al. (2015). We also employed multiple analytical approaches to demonstrate that the underlying broad signal in the NMR phosphomonoester region is not derived from a single molecule with a discrete molecular size, but rather from a continuum of unidentified P_{org} molecules spanning a wide molecular size distribution. This is in agreement with observations of McLaren et al. (2019) and Reusser et al. (2020b). In the four studied soils, broad signals were most prominent in the 10–20 and 20–50 kDa fractions rather than the highest molecular size fractions.

The number of underlying peaks necessary to account for the broad feature by spectral deconvolution fitting varied between soils and molecular size fractions. Previously, a single broad signal has been used to represent the 'unresolved' P_{org} pool (Reusser et al., 2020a). However, this approach results in an imperfect Lorentzian/Gaussian distribution, explaining the high variations of the C5 peak of *myo*-IP_6 in spectral deconvolution fitting results reported by Reusser et al. (2020a). Using a line width at half-height of 88 Hz in this study provides evidence for the existence of more than one underlying broad peak, suggesting the presence of several compounds. McLaren et al. (2019) reported that line widths at half-height of the fitted broad signal were on average 196 Hz. However, transverse relaxation times suggest the line widths are closer to 11 Hz. In addition, the underlying broad peak in the δ 4.5–4.0 ppm chemical shift region appears to be more pronounced compared to the fitted broad peaks closer to the side of the phosphomonoester region.

Table 4
Concentrations (mg P/kg_{soil}) of P species in each molecular size fraction as determined by solution ^{31}P NMR spectroscopy and spectral deconvolution fitting, as described in (Reusser et al., 2020a). Molecular size fractions were obtained on NaOH-EDTA soil extracts using high-resolution SEC (Superdex™ 75 prep grade column). Pools of 'Other IP_6' include the *neo* and *chiro* stereoisomers of IP_6. Pools of lower-order IP include *scyllo*-IP_5, *myo*-(1,2,4,5,6)-IP_5 and *scyllo*-IP_4. The concentrations of glycerophosphate include the unknown high molecular weight (HMW) P_{org} compound described by McLaren et al. (2015), whose peak overlaps with α-glycerophosphate. The proportion (%) of P to that of the $P_{tot,e}$ in each molecular size fraction is reported in parentheses. The < 5 kDa fractions do not include the removed fraction by the desalting process (Table SI-1).

	myo-IP_6	*scyllo*-IP_6	other IP_6	lower order IP	broad peaks	Glycerophosphate + HMW P_{org}
	(mg P/kg_{soil})	(mg P/kg_{soil})	(mg P/kg_{soil})	(mg P/kg_{soil})	(mg P/kg_{soil})	(mg P/kg_{soil})
Cambisol (P)						
<5 kDa	44.6	17.2	6.0	11.4	26.8 (23)	1.4
5–10 kDa	20.3	8.8	2.4	4.6	32.1 (41)	2.6
10–20 kDa	–	0.6	–	–	18.0 (67)	3.3
20–50 kDa	–	–	–	–	13.7 (66)	3.2
50->70 kDa*	–	0.3	–	–	9.1 (66)	3.4
Cambisol (F)						
<5 kDa	1.0	0.7	–	1.4	26.3 (62)	–
5–10 kDa	0.1	1.4	–	3.4	51.5 (64)	6.2
10–20 kDa	0.6	0.6	–	0.3	30.4 (76)	3.2
20–50 kDa	2.9	2.1	–	0.9	23.2 (64)	2.4
50–70 kDa	3.0	2.1	–	0.8	6.6 (43)	0.2
>70 kDa	8.1	9.4	–	3.1	21.5 (50)	–
Gleysol						
<5 kDa	50.5	23.1	7.8	7.5	25.7 (21)	–
5–10 kDa	33.1	13.1	1.7	5.0	33.3 (36)	–
10–20 kDa	0.7	1.6	–	–	27.5 (77)	2.5
20–50 kDa	1.2	2.4	–	–	34.0 (79)	4.1
50–70 kDa	1.9	1.5	0.2	–	16.6 (70)	2.8
>70 kDa	2.5	1.7	–	–	9.6 (65)	1.0
Cambisol (A)						
<5 kDa	1.9	2.8	–	–	13.7 (71)	–
5–10 kDa	2.0	1.7	–	2.0	17.6 (71)	–
10–20 kDa	–	0.1	–	–	11.8 (86)	1.7
20–50 kDa	–	–	–	–	14.5 (88)	2.0
50–70 kDa	–	–	–	–	8.1 (93)	2.4
>70 kDa	–	–	–	–	7.0 (95)	–

* The 50–70 kDa and > 70 kDa fractions of Cambisol (P) have been pooled. The given values represent the concentrations measured in the pooled fraction.

This could suggest that 1) the net peak area of sharp peaks arising from other phosphomonoesters in this region is influenced by the underlying broad signal; and 2) the restriction of the chemical shift region where most of the signal of the unresolved P_{org} pool appears will help to identify P containing molecular structures resonating in this specific region. In the former case, sharp peaks arising from other phosphomonoesters may be more susceptible to overestimation when any underlying broad signals are not accounted for in SDF procedures compared to other compounds at the side of the chemical shift region. The latter case could improve our understanding of the chemical nature of this pool in future studies.

The results of this study show that at least 32 % (Cambisol (P)) and as much as 93 % (Cambisol (F)) of total detected IP was present in molecular size fractions > 5 kDa. These findings are in agreement with other studies as Veinot and Thomas (1972), Hong and Yamane (1981) and Borie et al. (1989). Furthermore, we provide direct spectroscopic evidence that IP are present in large molecular size fractions of soil extracts as well as information on their speciation.

The mechanisms by which IP become associated with large molecules such as SOM and/or relatively small (nano-) sized soil minerals (Borie et al., 1989; Celi and Barberis, 2005; Moyer and Thomas, 1970; Omotoso and Wild, 1970) is assumed to be via metal bridges, presumably with Fe or Al (Veinot and Thomas, 1972; Vincent et al., 2012), or nucleophilic addition of free amine groups to aromatic rings (Borie et al., 1989). The occurrence of the latter mechanism during phosphorylation of model humic polymers was reported by Brannon and Sommers (1985). Cosgrove (1977) suggested that high molecular weight material consists of complexes of Fe(III) and nitrogenous organic matter containing IP_6. Another possibility could be that the phosphate groups of IP associate with SOM *via* ester-bonds, forming part of the SOM suprastructure model introduced by Piccolo (2001). Jørgensen et al. (2015) reported that the relative importance of the main binding sites (SOM matrix, amorphous metal oxides or clay minerals) in stabilising IP_6 can vary markedly between soils and that the association of IP_6 with SOM can be important in soils despite high contents of amorphous iron and aluminium oxides. The Cambisol (F) studied here has not only a high organic carbon content but also the highest amounts of oxalate extractable (amorphous) Fe and Al. Such findings emphasise that the mechanisms of incorporation of IP into large organic molecules and a possible role of IP in stabilising SOM, as proposed by Tipping et al. (2016), warrant further investigation. For example, one concern is that targeted degradation of the soil IP pool for the purpose of plant-nutrition could result in destabilisation of SOM structure.

In soils, the most abundant stereoisomers of IP_6 are *myo*-IP_6 (50 to 60 %) and *scyllo*-IP_6 (30 %), whereas *neo*-IP_6 (6%) and D-*chiro*-IP_6 (5 %) are less abundant forms (Irving and Cosgrove, 1982). In our study, the IP_6 pool in large molecular size fractions above 10 kDa of the Cambisol (F) and Gleysol is mainly composed of the *scyllo* (51 %) and *myo* (49 %) forms. The other stereoisomers comprised less than 1%. These findings suggest that *scyllo*-IP_6 could be more prone to associations with high molecular size compounds compared to other stereoisomers.

We present evidence that molecular size fractions > 5 kDa consist not only of IP_6, as previously proposed, but also of lower-order IP. *scyllo*-IP_5 was detected in all molecular size fractions of the Cambisol (F) soil extract, suggesting similar mechanisms of association to IP_6. Association of a proportion of IP with organic phases may limit not only the accessibility of IP_6 to enzymatic hydrolysis in soils, but also a fraction of lower-order IP. However, this is likely to depend on the stereochemistry of the associations, including the spatial protection conferred to IP, as well as whether IP is linked to the SOM matrix by metal bridges or ester bonds, which might be more readily hydrolysed by phosphatases.

Our findings regarding phospholipids and phosphodiesters in large

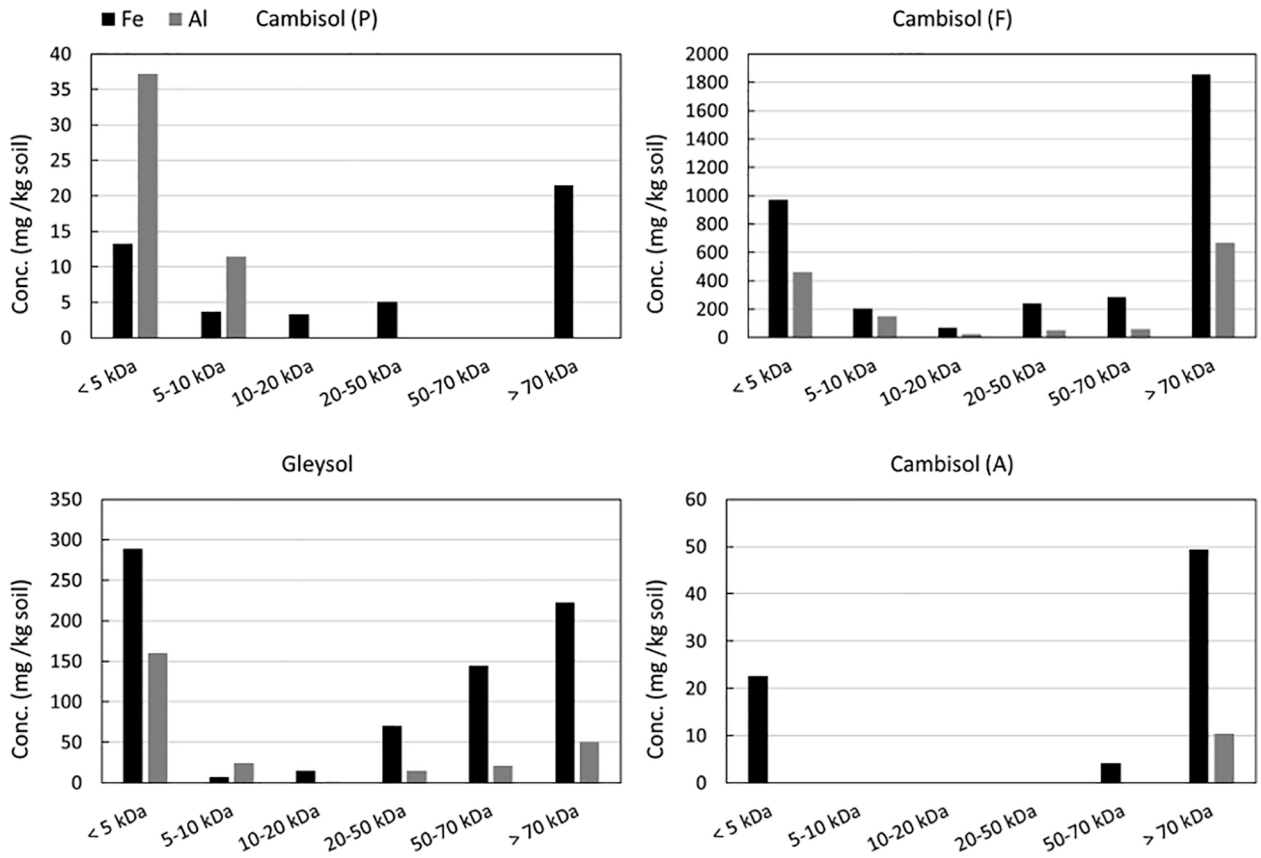

Fig. 3. Concentrations of aluminium (Al, grey) and iron (Fe, black) in 0.25 M NaOH + 0.05 M EDTA soil extracts following passage through a Superdex™ 75 prep grade column, which resulted in several technically defined fractions with molecular sizes of < 5, 5–10, 10–20, 20–50, 50–70, and > 70 kDa. Concentrations in the molecular size fractions were analysed by ICP-OES.

molecular size material are comparable with the studies of Missong et al. (2016) on forest soil colloids and Wang et al. (2017) using DOSY NMR spectroscopy of NaOH-EDTA soil extracts. The presence of glycerophosphates in large molecular size fractions could be explained by hydrolysis of large phospholipid molecules by NaOH (Doolette et al., 2011) or associations of glycerophosphates, which were intrinsically present in the soil sample (Wang et al., 2021), with large molecular size compounds. However, McLaren et al. (2015) reported the presence of a high molecular weight (> 10 kDa) P_{org} compound at a similar chemical shift to the α-glycerophosphate peak. We could not resolve these peaks in our spectra, hence the concentrations of glycerophosphate and this unknown high molecular weight compound are confounded. We assume that this compound, and not α-glycerophosphate, is mainly present in the Cambisol (F), Gleysol and Cambisol (A) soil samples due to the lack of the corresponding β-glycerophosphate peak.

Gerke (1992) proposed that a dominant proportion of soil P is present in the form of P_{inorg} (as orthophosphate) associated with organic molecules via metal bridges, i.e. Fe^{3+} and Al^{3+}, forming large molecules. The author states that often over 50 % of these associations may be hydrolysed during spectrophotometric determination of P_{org} and P_{inorg} using the phosphomolybdate method. Hence, P in these associations would be misattributed to the free orthophosphate pool. In our study, orthophosphate is present in large molecular size fractions but to a much lesser extent compared to the < 5 kDa fractions. The predominant proportion of P in large molecular size fractions is present as phosphomonoesters, and to a lesser extent phosphodiesters. We propose that 1) IP complexed by SOM and large molecular size material through metal bridges (Borie et al., 1989) and 2) P linked via ester bonds to the SOM organic molecules (McLaren et al., 2020; McLaren et al., 2015) contribute to the majority of large molecular size soil P.

5.3. Nuclear magnetic resonance observability

Few studies applying solution ^{31}P NMR spectroscopy of soil samples report the NMR observability as recommended by Doolette et al. (2011). In our previous studies on the same soil samples, NMR observability values ranged from 52 % to 94 % (Reusser et al., 2020a; Reusser et al., 2020b). Reduction of the NMR observability with increasing molecular size in this study could be related to an increase of precipitates at the bottom of the microcentrifuge tubes after centrifugation at 10621 *g*. Missong et al. (2016) used ultracentrifugation at 14,000 *g* for 60 min to separate water-dispersible colloids from the electrolyte phase. In our study, precipitation of colloids containing P not removed by filtration but by centrifugation could account for the low NMR observability of large molecular size material. To test this, we measured total P contents in the precipitates by total digestion and subsequent P analysis by ICP-OES. Results indicate that on average only 7 % (SD = 6 %) of $P_{tot,e}$, representing 4.5 mg P/kg_{soil} (SD = 3.6 mg P/kg_{soil}), was lost to precipitation. However, an exception was the > 70 kDa fraction of the Cambisol (F), which had a concentration of 121.3 mg P/kg_{soil} in the precipitate, representing 58 % of $P_{tot,e}$. This soil sample contains a large amount of amorphous and complexed Fe and Al oxides (Table 1) as well as a large amount of Fe in the largest molecular size fraction. The increase in the pH during sample preparation for NMR may have resulted in complex formation of IP and other P_{org} compounds with metals and organic matter, decreasing their solubility (Celi and Barberis, 2005; Hiradate et al., 2006; Martin and Evans, 1987). P concentrations in precipitates were correlated with NMR observability in the Cambisol (F) and Cambisol (A) but not in the Cambisol (P) and the Gleysol (Figure SI-12). Decreasing NMR observability with increasing molecular size due to precipitation suggests that quantification and identification of P

compounds in large molecular size material by solution ^{31}P NMR spectroscopy could be underestimated in some soils.

5.4. Metal concentrations in molecular size fractions

Multivalent cations, including Al^{3+} and Fe^{3+}, are known to form complexes with organic compounds possessing free electron pairs such as amines, carboxylates and ethers, as well as phosphate anions (Gerke, 2010; Parfitt, 1979; Stevenson, 1994; Turner et al., 2002; Vincent et al., 2012). In our study, Al was present mostly at elution volumes in the range of 1 kDa (single peak at $K_{av} = 0.7$, Figure SI-5). This large signal is assumed to arise from metal-EDTA complexes, EDTA being present in the extractant. We assume that most Zn and Al was either present in the free ion form or was liberated from soil compounds during extraction.

Concentrations of Fe were highest in the < 5 kDa and > 70 kDa molecular size fractions: the first pool is likely to be dominated by Fe-EDTA complexes; the second by Fe-oxyhydroxides or Fe bound to/complexed with oxygen containing organic compounds (Stevenson, 1994), based on their molecular sizes (Lead and Wilkinson, 2006). When converting molecular size in Da to the nm scale, a spherical molecule with a molecular size of 70 kDa would exhibit a minimum diameter of approximately 5.5 nm (Erickson, 2009). Fe-oxyhydroxides range from 1 nm to 1 μm in size (Lead and Wilkinson, 2006). The high Fe concentration in the > 70 kDa fraction of the Cambisol (F) could also indicate the presence of P_{org} adsorbed to Fe oxyhydroxide nanoparticles (Lead and Wilkinson, 2006; Missong et al., 2016; Ognalaga et al., 1994) or P_{org} complexed with Fe^{3+}. These hypotheses are supported by the positive correlation of IP concentrations in the size fractions of the Cambisol (F) sample with measured Fe. Celi and Barberis (2005) reported that indirect adsorption of P_{org} through bi- or trivalent cations with the resulting formation of ternary organic matter-metal-P complexes is one abiotic process which contributes to incorporation of P_{org} into SOM. Furthermore, Fe oxides were identified as important sorbents of organic matter and thus playing a major role in controlling long-term SOM preservation (Kögel-Knabner et al., 2008).

The differing molecular size distributions of Fe and Al apparent in our chromatograms indicate that total soil concentrations of Al and Fe do not reflect the abundance of larger molecular size complexes containing P and that the association of P_{org} with Al in large molecular size complexes is less important than its association with Fe. Further research is needed to understand the association of P_{inorg} and P_{org} with Fe and Al in large molecular size material to elucidate the stability and cycling of these complexes in soil systems.

6. Conclusion

The majority of P_{org} in soil extracts are associated with molecules > 5 kDa in size. We report for the first time the presence of *myo* and *scyllo* stereoisomers of IP_6, as well as some lower-order IP species, in molecular sized material above 5 kDa by combining high-resolution size exclusion chromatography and solution ^{31}P NMR spectroscopy. We provide confirmatory evidence for an uncharacterised P_{org} pool in soil being responsible for poorly resolved broad signals in the phosphomonoester region of soil extracts. The largest pool of P_{org} associated with these large molecules is generally represented by three or four underlying broad signals in the phosphomonoester region of NMR spectra. This uncharacterised pool of phosphomonoesters contains several components rather than single polymers of discrete molecular sizes. The corresponding NMR signal is comprised of several overlapping broad peaks with varying peak shapes and line widths, indicating diverse compositions of the high molecular size P_{org} pool. This P_{org} pool is represented by P_{org}-SOM associations rather than orthophosphate adsorbed to organic molecules via metal bridges. Metals, particularly Fe, appear to be an important bridging component of P_{org} associations in the largest molecular size material. The findings of this study will contribute to our understanding of P_{org}-SOM associations and their importance in the soil P cycle. Improved understanding of the structural composition and associations of the abundant unresolved P_{org} pool is necessary for further studies investigating mineralisation processes targeting this pool for plant nutrition purposes and/or P stabilisation processes in soil systems.

Declaration of Competing Interest

The authors declare that they have no known competing financial interests or personal relationships that could have appeared to influence the work reported in this paper.

Acknowledgments

We greatly acknowledge the technical support of Dr Mark Durenkamp and advice from Dr Caterina Dell'Aquila at Rothamsted Research, and Dr Laurie Schönholzer at the ETH Zurich. Furthermore, we are very thankful for the soil samples provided by Dr Astrid Oberson, Dr David Lester, Dr Chiara Pistocchi and Dr Gregor Meyer.

Funding: This work was supported by the Swiss National Science Foundation (grant number 200021_169256). Andrew L. Neal was supported by the United Kingdom's Biotechnology and Biological Science Research Council-funded Soil to Nutrition strategic program (BBS/E/C/000I0310).

Appendix A. Supplementary data

Supplementary data to this article can be found online at https://doi.org/10.1016/j.geoderma.2022.115716.

References

Anderson, G., 1980. Assessing organic phosphorus in soils. In: Khasawneh, F.E., Sample, E.C., Kamprath, E.J. (Eds.), The role of phosphorus in agriculture. American Society of Agronomy, Crop Science Society of America, Soil Science Society of America, Madison, WI, pp. 411–431.

Anderson, G., Malcolm, R.E., 1974. The nature of alkali-soluble soil organic phosphates. J. Soil Sci. 25 (3), 282–297.

Annaheim, K.E., Doolette, A.L., Smernik, R.J., Mayer, J., Oberson, A., Frossard, E., Bünemann, E.K., 2015. Long-term addition of organic fertilizers has little effect on soil organic phosphorus as characterized by ^{31}P NMR spectroscopy and enzyme additions. Geoderma 257-258, 67–77.

Auten, J.T., 1923. Organic phosphorus of soils. Soil Sci. 16 (4), 281. https://doi.org/10.1097/00010694-192310000-00006.

Bloembergen, N., Purcell, E.M., Pound, R.V., 1948. Relaxation effects in nuclear magnetic resonance absorption. Phys. Rev. 73 (7), 679–712.

Borie, F., Zunino, H., Martínez, L., 1989. Macromolecule-P associations and inositol phosphates in some chilean volcanic soils of temperate regions. Commun. Soil Sci. Plant Anal. 20 (17-18), 1881–1894.

Bowman, R.A., Moir, J.O., 1993. Basic EDTA as an extractant for soil organic phosphorus. Soil Sci. Soc. Am. J. 57 (6), 1516–1518.

Brannon, C.A., Sommers, L.E., 1985. Preparation and characterization of model humic polymers containing organic phosphorus. Soil Biol. Biochem. 17 (2), 213–219.

Bünemann, E.K., Smernik, R.J., Marschner, P., McNeill, A.M., 2008. Microbial synthesis of organic and condensed forms of phosphorus in acid and calcareous soils. Soil Biol. Biochem. 40 (4), 932–946.

Cade-Menun, B.J., 2015. Improved peak identification in ^{31}P-NMR spectra of environmental samples with a standardized method and peak library. Geoderma 257-258, 102–114.

Cade-Menun, B.J., Liu, C.W., Nunlist, R., McColl, J.G., 2002. Soil and litter phosphorus-31 nuclear magnetic resonance spectroscopy. J. Environ. Qual. 31 (2), 457–465.

Celi, L., Barberis, E., 2005. Abiotic stabilisation of organic phosphorus in the environment. In: Turner, B.L., Frossard, E., Baldwin, D.S. (Eds.), Organic phosphorus in the environment. CABI Publishing, Wallingford, UK, pp. 113–132.

Celi, L., Barberis, E., 2007. Abiotic reactions of inositol phosphates in soil. In: Turner, B. L., Richardson, A.E., Mullaney, E.J. (Eds.), Inositol phosphates: linking agriculture and the environment. CABI, Wallingford, pp. 207–220.

Cosgrove, D.J., 1977. Microbial transformations in the phosphorus cycle. In: Alexander, M. (Ed.), Advances in Microbial Ecology. Springer, US, Boston, MA, pp. 95–134.

Dalal, R.C., 1977. Soil organic phosphorus. In: Brady, N.C. (Ed.), Advances in Agronomy. Academic Press, pp. 83–117.

Dell'Aquila, C., Neal, A.L., Shewry, P.R., 2020. Development of a reproducible method of analysis of iron, zinc and phosphorus in vegetables digests by SEC-ICP-MS. Food Chem. 308, 125652. https://doi.org/10.1016/j.foodchem.2019.125652.

Doolette, A.L., Smernik, R.J., 2011. Soil organic phosphorus speciation using spectroscopic techniques. In: Bünemann, E., Oberson, A., Frossard, E. (Eds.),

Phosphorus in action: biological processes in soil phosphorus cycling. Springer, Berlin Heidelberg, Berlin, Heidelberg, pp. 3–36.
Doolette, A.L., Smernik, R.J., Dougherty, W.J., 2011. Overestimation of the importance of phytate in NaOH–EDTA soil extracts as assessed by ^{31}P NMR analyses. Org Geochem. 42 (8), 955–964.
Dougherty, W.J., Smernik, R.J., Bünemann, E.K., Chittleborough, D.J., 2007. On the use of hydrofluoric acid pretreatment of soils for phosphorus-31 nuclear magnetic resonance analyses. Soil Sci. Soc. Am. J. 71 (4), 1111–1118.
Dougherty, W.J., Smernik, R.J., Chittleborough, D.J., 2005. Application of spin counting to the solid-state ^{31}P NMR analysis of pasture soils with varying phosphorus content. Soil Sci. Soc. Am. J. 69 (6), 2058–2070.
Erickson, H.P., 2009. Size and shape of protein molecules at the nanometer level determined by sedimentation, gel filtration, and electron microscopy. Biological Procedures Online 11 (1), 32–51.
Fioroto, A.M., Kelmer, G.A.R., Albuquerque, L.G.R., César Paixão, T.R.L., Oliveira, P.V., 2017. Microwave-assisted digestion with a single reaction chamber for mineral fertilizer analysis by inductively coupled plasma optical emission spectrometry. Spectrosc. Lett. 50 (10), 550–556.
Gerke, J., 1992. Orthophosphate and organic phosphate in the soil solution of four sandy soils in relation to pH-evidence for humic-FE-(AL-) phosphate complexes. Commun. Soil Sci. Plant Anal. 23 (5-6), 601–612.
Gerke, J., 2010. Humic (organic matter)-Al(Fe)-phosphate complexes: an underestimated phosphate form in soils and source of plant-available phosphate. Soil Sci. 175 (9), 417–425.
Gottselig, N., Nischwitz, V., Meyn, T., Amelung, W., Bol, R., Halle, C., Vereecken, H., Siemens, J., Klumpp, E., 2017. Phosphorus binding to nanoparticles and colloids in forest stream waters. Vadose Zone Journal 16(3), vzj2016.2007.0064.
Harrison, A.F., 1982. ^{32}P-method to compare rates of mineralization of labile organic phosphorus in woodland soils. Soil Biol. Biochem. 14 (4), 337–341.
Harrison, H.F., 1987. Soil organic phosphorus: a review of world literature. CAB International, Wallingford.
Hens, M., Merckx, R., 2001. Functional characterization of colloidal phosphorus species in the soil solution of sandy soils. Environmental Science & Technology 35 (3), 493–500.
Hiradate, S., Yonezawa, T., Takesako, H., 2006. Isolation and purification of hydrophilic fulvic acids by precipitation. Geoderma 132 (1-2), 196–205.
Hong, J.-K., Yamane, I., 1981. Distribution of inositol phosphate in the molecular size fractions of humic and fulvic acid fractions. Soil Science and Plant Nutrition 27 (3), 295–303.
Irving, G.C.J., Cosgrove, D.J., 1982. The use of gas-liquid chromatography to determine the proportions of inositol isomers present as pentakis- and hexakisphosphates in alkaline extracts of soils. Commun. Soil Sci. Plant Anal. 13 (11), 957–967.
Jarosch, K.A., Doolette, A.L., Smernik, R.J., Tamburini, F., Frossard, E., Bünemann, E.K., 2015. Characterisation of soil organic phosphorus in NaOH-EDTA extracts: a comparison of ^{31}P NMR spectroscopy and enzyme addition assays. Soil Biol. Biochem. 91, 298–309.
Jørgensen, C., Turner, B.L., Reitzel, K., 2015. Identification of inositol hexakisphosphate binding sites in soils by selective extraction and solution ^{31}P NMR spectroscopy. Geoderma 257-258, 22–28.
Keeler, J., 2010. Understanding NMR spectroscopy, 2nd ed. Wiley-Blackwell, Chichester.
Kögel-Knabner, I., Guggenberger, G., Kleber, M., Kandeler, E., Kalbitz, K., Scheu, S., Eusterhues, K., Leinweber, P., 2008. Organo-mineral associations in temperate soils: integrating biology, mineralogy, and organic matter chemistry. J. Plant Nutr. Soil Sci. 171 (1), 61–82.
Kögel-Knabner, I., Rumpel, C., 2018. Chapter One - Advances in molecular approaches for understanding soil organic matter composition, origin, and turnover: a historical overview. In: Sparks, D.L. (Ed.), Advances in Agronomy. Academic Press, pp. 1–48.
Lead, J.R., Wilkinson, K.J., 2006. Aquatic colloids and nanoparticles: current knowledge and future trends. Environ. Chem. 3 (3), 159–171.
Lévesque, M., 1969. Characterization of model and soil organic matter metal-phosphate complexes. Can. J. Soil Sci. 49 (3), 365–373.
Lévesque, M., Schnitzer, M., 1967. Organo-metallic interactions in soils: 6. Preparation and properties of fulvic acid-metal phosphates. Soil Sci. 103 (3), 183–190.
Martin, C.J., Evans, W.J., 1987. Phytic acid: divalent cation interactions. V. titrimetric, calorimetric, and binding studies with cobalt(ii) and nickel(ii) and their comparison with other metal ions. J. Inorg. Biochem. 30 (2), 101–119.
McLaren, T.I., Smernik, R.J., McLaughlin, M.J., Doolette, A.L., Richardson, A.E., Frossard, E., 2020. Chapter Two - The chemical nature of soil organic phosphorus: a critical review and global compilation of quantitative data. In: Sparks, D.L. (Ed.), Advances in Agronomy. Academic Press, pp. 51–124.
McLaren, T.I., Smernik, R.J., McLaughlin, M.J., McBeath, T.M., Kirby, J.K., Simpson, R. J., Guppy, C.N., Doolette, A.L., Richardson, A.E., 2015. Complex forms of soil organic phosphorus–A major component of soil phosphorus. Environ. Sci. Technol. 49 (22), 13238–13245.
McLaren, T.I., Verel, R., Frossard, E., 2019. The structural composition of soil phosphomonoesters as determined by solution ^{31}P NMR spectroscopy and transverse relaxation (T_2) experiments. Geoderma 345, 31–37.
Meyer, G., Bünemann, E.K., Frossard, E., Maurhofer, M., Mäder, P., Oberson, A., 2017. Gross phosphorus fluxes in a calcareous soil inoculated with Pseudomonas protegens CHA0 revealed by ^{33}P isotopic dilution. Soil Biol. Biochem. 104, 81–94.
Missong, A., Bol, R., Willbold, S., Siemens, J., Klumpp, E., 2016. Phosphorus forms in forest soil colloids as revealed by liquid-state ^{31}P-NMR. J. Plant Nutr. Soil Sci. 179 (2), 159–167.
Moyer, J.R., Thomas, R.L., 1970. Organic phosphorus and inositol phosphates in molecular size fractions of a soil organic matter extract. Soil Sci. Soc. Am. J. 34 (1), 80–83.
Nebbioso, A., Piccolo, A., 2012. Advances in humeomics: Enhanced structural identification of humic molecules after size fractionation of a soil humic acid. Anal. Chim. Acta 720, 77–90.
Newman, R.H., Tate, K.R., 1980. Soil phosphorus characterisation by ^{31}P nuclear magnetic resonance. Commun. Soil Sci. Plant Anal. 11 (9), 835–842.
Ognalaga, M., Frossard, E., Thomas, F., 1994. Glucose-1-phosphate and *myo*-inositol hexaphosphate adsorption mechanisms on goethite. Soil Sci. Soc. Am. J. 58 (2), 332–337.
Ohno, T., Zibilske, L.M., 1991. Determination of low concentrations of phosphorus in soil extracts using malachite green. Soil Sci. Soc. Am. J. 55 (3), 892–895.
Omotoso, T.I., Wild, A., 1970. Occurence of inositol phosphates and other organic phosphate components in an organic complex. J. Soil Sci. 21 (2), 224–232.
Pansu, M., Gautheyrou, J. (Eds.), 2006. Handbook of Soil Analysis. Springer Berlin Heidelberg, Berlin, Heidelberg.
Parfitt, R.L., 1979. Anion adsorption by soils and soil materials. In: Brady, N.C. (Ed.), Advances in Agronomy. Academic Press, pp. 1–50.
Piccolo, A., 2001. The supramolecular structure of humic substances. Soil Sci. 166 (11), 810–832.
R Core Team, 2020. R: A language and environment for statistical computing. In: R.F.f.S. Computing (Ed.), Vienna, Austria.
Reusser, J.E., Verel, R., Frossard, E., McLaren, T.I., 2020a. Quantitative measures of *myo*-IP_6 in soil using solution ^{31}P NMR spectroscopy and spectral deconvolution fitting including a broad signal. Environ. Sci. Processes Impacts 22 (4), 1084–1094.
Reusser, J.E., Verel, R., Zindel, D., Frossard, E., McLaren, T.I., 2020b. Identification of lower-order inositol phosphates (IP_5 and IP_4) in soil extracts as determined by hypobromite oxidation and solution ^{31}P NMR spectroscopy. Biogeosciences 17 (20), 5079–5095.
Schwertmann, U., 1964. Differenzierung der Eisenoxide des Bodens durch Extraktion mit Ammoniumoxalat-Lösung. Zeitschrift für Pflanzenernährung, Düngung, Bodenkunde 105 (3), 194–202.
Spain, A.V., Tibbett, M., Ridd, M., McLaren, T.I., 2018. Phosphorus dynamics in a tropical forest soil restored after strip mining. Plant Soil 427 (1-2), 105–123.
Stevenson, F.J., 1994. Humus chemistry: genesis, composition, reactions, Second ed. Wiley, New York [etc.].
Steward, J.H., Tate, M.E., 1971. Gel chromatography of soil organic phosphorus. J. Chromatogr. A 60, 75–82.
Tamburini, F., Pistocchi, C., Helfenstein, J., Frossard, E., 2018. A method to analyse the isotopic composition of oxygen associated with organic phosphorus in soil and plant material. Eur. J. Soil Sci. 69 (5), 816–826.
Tipping, E., Somerville, C.J., Luster, J., 2016. The C:N:P: S stoichiometry of soil organic matter. Biogeochemistry 130 (1-2), 117–131.
Turner, B.L., 2008. Soil organic phosphorus in tropical forests: an assessment of the NaOH–EDTA extraction procedure for quantitative analysis by solution ^{31}P NMR spectroscopy. Eur. J. Soil Sci. 59 (3), 453–466.
Turner, B.L., Cheesman, A.W., Godage, H.Y., Riley, A.M., Potter, B.V., 2012. Determination of *neo*- and D-*chiro*-inositol hexakisphosphate in soils by solution ^{31}P NMR spectroscopy. Environ Sci Technol 46 (9), 4994–5002.
Turner, B.L., Mahieu, N., Condron, L.M., 2003. Quantification of *myo*-inositol hexakisphosphate in alkaline soil extracts by solution ^{31}P spectroscopy and spectral deconvolution. Soil Sci. 168 (7), 469–478.
Turner, B.L., Papházy, M.J., Haygarth, P.M., Mckelvie, I.D., 2002. Inositol phosphates in the environment. Philos. Trans. R. Soc. Lond. B Biol. Sci. 357 (1420), 449–469.
Turner, B.L., Richardson, A.E., 2004. Identification of *scyllo*-inositol phosphates in soil by solution phosphorus-31 nuclear magnetic resonance spectroscopy. Soil Sci. Soc. Am. J. 68 (3), 802–808.
Veinot, R.L., Thomas, R.L., 1972. High molecular weight organic phosphorus complexes in soil organic matter: inositol and metal content of various fractions. Soil Sci. Soc. Am. J. 36 (1), 71–73.
Vestergren, J., Vincent, A.G., Jansson, M., Persson, P., Ilstedt, U., Gröbner, G., Giesler, R., Schleucher, J., 2012. High-resolution characterization of organic phosphorus in soil extracts using 2D ^{1}H–^{31}P NMR correlation spectroscopy. Environ. Sci. Technol. 46 (7), 3950–3956.
Vincent, A.G., Schleucher, J., Gröbner, G., Vestergren, J., Persson, P., Jansson, M., Giesler, R., 2012. Changes in organic phosphorus composition in boreal forest humus soils: the role of iron and aluminium. Biogeochemistry 108 (1-3), 485–499.
Vold, R.L., Waugh, J.S., Klein, M.P., Phelps, D.E., 1968. Measurement of spin relaxation in complex systems. J. Chem. Phys. 48 (8), 3831–3832.
Wang, L., Amelung, W., Willbold, S., 2017. Diffusion-Ordered Nuclear Magnetic Resonance Spectroscopy (DOSY-NMR): A Novel Tool for Identification of Phosphorus Compounds in Soil Extracts. Environ. Sci. Technol. 51 (22), 13256–13264.
Wang, L., Amelung, W., Willbold, S., 2021. ^{18}O isotope labeling combined with ^{31}P nuclear magnetic resonance spectroscopy for accurate quantification of hydrolyzable phosphorus species in environmental samples. Anal. Chem. 93 (4), 2018–2025.
WRB, I.W.G., 2014. World reference base for soil resources. International soil classification system for naming soils and creating legends for soil maps. World Soil Resources Reports No. 106. Food and Agriculture Organization of the United Nations FAO, Rome.